Organic Electronics 12 (2011) 2065–2070

Contents lists available at SciVerse ScienceDirect

Organic Electronics

journal homepage: www.elsevier.com/locate/orgel

Alleviate microcavity effects in top-emitting white organic light-emitting diodes for achieving broadband and high color rendition emission spectra

Shuming Chen, Hoi-Sing Kwok *

Center for Display Research, Department of Electronic and Computer Engineering, The Hong Kong University of Science and Technology, Clear Water Bay, Kowloon, Hong Kong

ARTICLE INFO

Article history:
Received 25 July 2011
Received in revised form 21 August 2011
Accepted 22 August 2011
Available online 9 September 2011

Keywords:
Top-emitting
White organic light-emitting diodes
Microcavity
Multiple emission peaks
High color rendering index
Microdisplay

ABSTRACT

It is challenging to obtain broadband emission spectra in top-emitting white organic light-emitting diodes (WOLEDs) due to the well known microcavity effects. In this work, we demonstrate that the microcavity effects can be greatly alleviated by employing a low reflection tri-cathode-layer Yb (5 nm)/Au (15 nm)/MoO_3 (35 nm). Top-emitting WOLEDs with evenly separated red, green and blue emission peaks have been achieved. The white emission spectra show weak angle dependence as well. At a luminance of 1000 cd/m^2, the top-emitting WOLEDs show an efficiency of 23 cd/A, 10.5 lm/W, a 1931 Commission International de L'Eclairage coordinate of (0.36, 0.42) and a high color rendering index of 85. The top-emitting WOLEDs have been successfully applied in the Si based microdisplay.

1. Introduction

White organic light-emitting diodes (WOLEDs) have received intensive study recently due to their potential applications in full color display and solid-state lighting [1,2]. In high resolution full color display such as the Si based microdisplay, the resolution typically is higher than SVGA+ and the sub-pixel size is smaller than 5×15 μm [3]; it is thus unpractical to realize full color microdisplay by laterally depositing the red (R), green (G) and blue (B) emission layers using fine metal shadow mask due to the difficulty of manufacturing, maintaining and aligning the shadow mask with tiny pixel pitch [4]. Therefore, it is more desirable to adopt the unpatterned WOLEDs combined with patterned RGB color filters to generate the three primary colors [5–7]. For microdisplay applications, the WOLEDs are required to be integrated on opaque Si based complementary metal-oxide semiconductor (CMOS) backplane. Thus one has to develop the top-emitting WOLEDs with a reflective bottom electrode and a semitransparent top electrode to force the light emitting from the top surface. The top-emitting WOLEDs should possess broadband emission spectra with three evenly separated R, G and B peaks so that the output white light can be separated into three primary colors after passing through the color filters. However, it is challenging to obtain the top-emitting WOLEDs with broadband spectra due to the well known microcavity effects which shape and narrow the emission spectra [5,6,8]. To alleviate the microcavity effects presented between two reflective electrodes, one has to reduce the reflection of either electrode. Many approaches have been proposed to achieve a low reflection electrode, for example, adopting a semitransparent Ca/Ag or LiF/Al/Ag cathode capped with an index matching layer [7,9–13], employing a transparent indium-tin-oxide top electrode [14], or using a low reflection anode material like Mo [15] or Cu [16]. Although top-emitting WOLEDs have been successfully demonstrated by employing the above-mentioned low reflection electrodes, the spectra or

* Corresponding author.
E-mail addresses: smchen@ust.hk (S. Chen), eekwok@ust.hk (H.-S. Kwok).

1566-1199/$ - see front matter © 2011 Elsevier B.V. All rights reserved.
doi:10.1016/j.orgel.2011.08.014

efficiency remain unsatisfied for high color gamut full color display or high color rendition illumination applications.

Au, one of the metals with low absorption, low reflection and high transmission, would be potentially an ideal cathode material for top-emitting WOLEDs [17]. However, few works have been reported on using Au as a low reflection and semitransparent cathode for top-emitting WOLEDs [18], mainly due to the high work function (~5.1 eV) of Au, rendering it unsuitable as a cathode material for injecting electrons. In this work, we demonstrate that with a 5 nm Yb (Ytterbium) modification layer, Au can be an excellent cathode for injecting electrons. The Au based tri-cathode-layer Yb (5 nm)/Au (15 nm)/MoO_3 (35 nm) exhibits an average reflection of 9.8% over the visible wavelength, significantly lower than 24% for the Ag based tri-cathode-layer Yb (5 nm)/Ag (15 nm)/MoO_3 (30 nm). By employing the low reflection Au based tri-cathode-layer, the microcavity effects have been weakened largely. Thus, high efficiency and high color rendition top-emitting WOLEDs with evenly separated R, G and B emission peaks have been achieved. At a high luminance of 1000 cd/m^2, the top-emitting WOLEDs exhibit an efficiency of 23 cd/A, 10.5 lm/W, a 1931 Commission International de L'Eclairage (CIE) coordinate of (0.36, 0.42) and a high color rendering index (CRI) of 85. The top-emitting WOLEDs demonstrated here would be an ideal candidate for high resolution full color active-matrix display or indoor lighting applications.

2. Experimental

Bis(3,5-difluoro-2-(2-pyridyl)phenyl)-(2-carboxypyridyl) iridium(III), FIrPic, and bis(2-benzo[*b*]thiophen-2-yl-pyridine)(acetylacetonate)iridium(III), Ir(btp)$_2$(acac) with main emission peak at 475 and 612 nm were selected as sky blue and saturated red emitter, respectively. In order to generate the white spectra with three evenly separated R, G and B emission peaks, a new yellowish-green emitter bis(5-(trifluoromethyl)-2-*p*-tolylpyridine) (acetylacetonate)iridium(III) **1** with emission peak at 544 nm was specially designed and employed in this study [1]. The top-emitting WOLEDs were fabricated in a multi-source vacuum chamber at a base pressure of around 5×10^{-7} Torr with structure glass/Al (100 nm)/MoO_3 (8 nm)/NPB (20, 30, 40 nm)/6% Ir(btp)$_2$(acac):CDBP (10 nm)/4% **1**:CDBP (3 nm)/12% FIrPic:CDBP (5 nm)/TAZ (40 nm)/Yb 5 nm/Au (or Ag) (15 nm)/MoO_3 (35, 30 nm), (NPB: *N*,*N*′-bis(naphthalen-1-yl)-*N*,*N*′-bis(phenyl)-benzidine; CDBP: 4,4′-bis(carbazol-9-yl)-2,2′-dimethylbiphenyl; TAZ: 3-(4-biphenyl)-4-phenyl-5-*tert*-butylphenyl-1,2,4-triazole), where Al, MoO_3 and NPB function as reflective anode, hole-injection and hole-transporting layer, respectively, CDBP works as host, TAZ serves as exciton-blocking and electron-transporting layer, Yb/Au (or Ag)/MoO_3 acts as semitransparent tri-cathode-layer. The energy level and molecular structure of the emitters are shown in Fig. 1. The transmission and reflection spectra of the tri-cathode-layer were characterized by UV–Vis spectrophotometer. The current density–voltage–luminance characteristics of the devices were measured by the HP4145B semiconductor parameter analyzer and a calibrated UDT PIN-25D silicon photodiode. The electroluminescent (EL) spectra were obtained with the PR650 spectrophotometer.

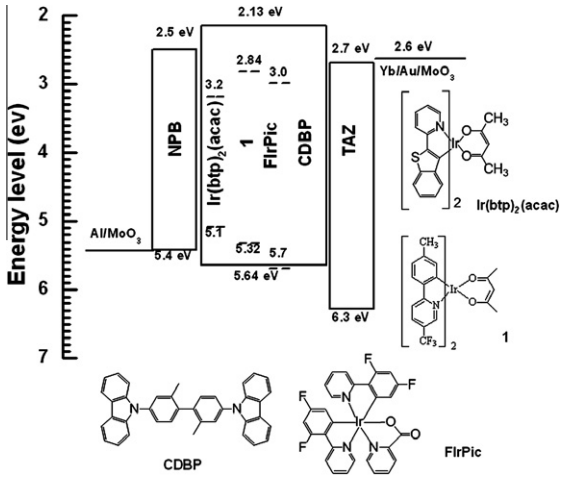

Fig. 1. Energy level and molecular structure of the materials employed in this study. The values of energy level are taken from literature.

3. Results and discussion

To alleviate the microcavity effects of the top-emitting WOLEDs, important parameters which affect the interference are analyzed first. The top-emitting OLEDs with the emission layers sandwiched between two reflective metal electrodes can be treated as a Fabry–Perot cavity optically [8,9,13,19–22]. Light emitting from the top semitransparent electrode and light reflected by the bottom reflective electrode interfere with each other. The emission intensity at λ is enhanced when the cavity effective length L_{eff} satisfies the below equation [8,20]:

$$L_{eff} = \frac{(\phi_{tm} + \phi_{bm})\lambda}{4\pi} + \sum_i n_i d_i = m\frac{\lambda}{2}\ (m:\ \text{integer}), \qquad (1)$$

where ϕ_{tm} and ϕ_{bm} are the phase shift of the light reflected by the top and bottom electrode, respectively; n_i and d_i are the refractive index and thickness of the organic layers, respectively. The cavity behaves like an optical filter which modulates the free space emission with the modulation spectra given by [8,13,19–21]:

$$I_{cav}(\lambda) \propto \frac{1 + R_1 + 2\sqrt{R_1}\cos\left(\frac{4\pi L_1}{\lambda} + \phi_{bm}\right)}{1 + R_1R_2 - 2\sqrt{R_1R_2}\cos\left(\frac{4\pi L}{\lambda} + \phi_{bm} + \phi_{tm}\right)} T_2, \qquad (2)$$

where L_1 is the optical distance between the exciton main recombination zone and the bottom reflective electrode; L is optical length of the organic layers; R_1 and R_2 are the reflectance of the bottom and top electrode, respectively; T_2 is the transmittance of the top electrode. The full width at half maximum (FWHM) of the $I_{cav}(\lambda)$ can be estimated by [8,9,13]:

$$\text{FWHM} = \frac{\lambda^2}{2L_{eff}} \times \frac{1 - \sqrt{R_1R_2}}{\pi\sqrt[4]{R_1R_2}}, \qquad (3)$$

From Eq. (3), one can see that larger reflectance of either electrode results in smaller FWHM, implying a stronger interference presented in the cavity. In order to obtain

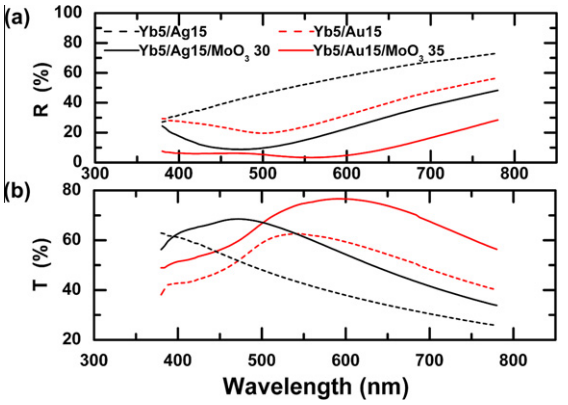

Fig. 2. Reflection (a) and transmission (b) spectra of the Ag and Au based semitransparent cathodes as measured by UV–VIS spectrometer.

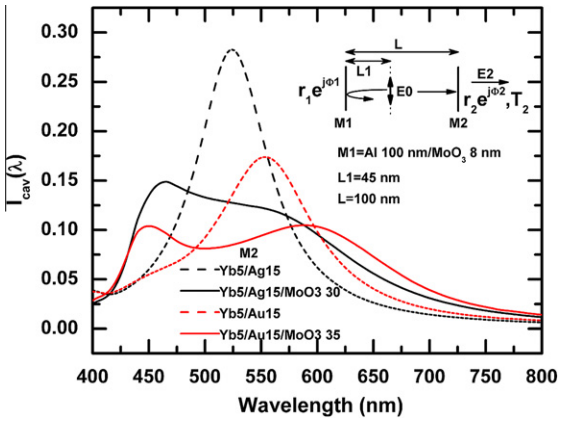

Fig. 3. Simulated cavity modulation spectra. Inset shows the physical model used in the simulation. The reflectance, phase shift and transmistance of the bottom anode $M1$ = Al 100 nm/MoO_3 8 nm and top cathode $M2$ are calculated by the transfer matrix method. The refractive indexes of the materials employed are taken from literature.

broadband emission spectra, one has to maximize the FWHM by reducing the reflection of either electrode. It is more desirable to reduce the reflection of the top electrode, since reducing the reflection of the bottom electrode, though effective, are at a cost of decreasing the light coupling efficiency.

Among the metal materials, thin film of Ag and Au are two mostly selected semitransparent top electrode materials due to their intrinsically low absorption and high transmission. Fig. 2 compares the measured reflection and transmission spectra of the Ag and Au based semitransparent top cathodes. It can be seen that the Au based top cathodes exhibit a substantially lower reflection over the visible wavelength than that of the Ag. Also, at yellow to red color, the transmittance of the Au based top cathodes is higher than that of the Ag based top cathodes. For example, the average reflectance (transmittance) of Yb (5 nm)/Au (15 nm) is 34% (52%), significantly lower (higher) than 54% (42%) for Yb (5 nm)/Ag (15 nm). By capping the semitransparent top cathodes with an index matching layer with optimized thickness, the reflectance (transmittance) of the Au and Ag based top cathodes are further reduced (enhanced). For example, the average reflectance (transmittance) has been remarkably reduced (enhanced) from 34% (52%) for the Au top cathodes without index matching layer to 9.8% (66%) for the Au top cathodes with 35 nm MoO_3 index matching layer. The low reflection of Yb (5 nm)/Au (15 nm)/MoO_3 (35 nm) suggests a good possibility of achieving a weakened interference cavity, and hence top-emitting WOLEDs with broadband emission spectra may be expected by employing this low reflection top cathode.

To evaluate the interference effects of the cavity with the low reflection top cathodes, cavity modulation spectra $I_{cav}(\lambda)$ are simulated. Although Eq. (2) provides a simple calculation formulation for $I_{cav}(\lambda)$, important parameters like dipole orientation, ***s***, ***p*** polarization, light emitting angles, exciton recombination zone and diffusing length are omitted. It is thus inaccurate to use Eq. (2) to describe the optical characteristics of the cavity. A rigorous electromagnetic modeling is adopted to accurately simulate the modulation spectra of the cavity [22]. Fig. 3 inset shows the physical model used in the simulation. Organic layers with thickness of L = 100 nm are sandwiched between the bottom reflective anode $M1$ = Al (100 nm)/MoO_3 (8 nm) and top semitransparent cathode $M2$. The distance between the exciton main recombination zone and the bottom anode is assumed to be $L1$ = 45 nm. The exciton diffusing length is assumed to be 15 nm. The reflectance, transmittance and phase shift of $M1$, $M2$ are calculated by the transfer matrix method by considering ***s***, ***p*** polarization. The modulation spectra of the cavity with different $M2$ are shown in Fig. 3. It can be clearly seen that with lower reflection $M2$, the modulation spectra exhibit wider FWHM. For example, with $M2$ = Yb (5 nm)/Ag (15 nm), the spectra exhibit a clear interference peak at 525 nm and a FWHM of only 78 nm; thus it is unlikely to obtain broadband white emission spectra in such cavity due to strong modulation of the cavity at green color. While by replacing Ag with low reflection Au, the intensity of the interference peak is suppressed and the FWHM is broadened to 110 nm. Further capping an optimized index matching layer reduces the reflection of $M2$ and broadens the FWHM accordingly. For example, the FWHM is broadened to 194 nm and 256 nm for $M2$ = Yb (5 nm)/Ag (15 nm)/MoO_3 (30 nm) and $M2$ = Yb (5 nm)/Au (15 nm)/MoO_3 (35 nm), respectively. Due to alleviation of the interference, the cavity with $M2$ = Yb (5 nm)/Au (15 nm)/MoO_3 (35 nm) exhibits a rather flat modulation intensity from 440 to 600 nm, implying a good possibility of obtaining broadband white emission spectra with equal R, G and B intensity in such cavity.

To verify this assertion, top-emitting WOLEDs with different top cathodes were fabricated. Fig. 4 shows the EL spectra of the devices with different top cathodes. For devices with Yb (5 nm)/Ag (15 nm) cathode, due to strong interference at λ = 525 nm as predicted by the simulated cavity modulation spectra, the green emission is enhanced significantly while the blue and red emission are suppressed, resulting in unbalanced white spectra as shown in Fig. 4a inset. For the devices with Ag and Au based tri-cathode-layer, the cavity length was tuned deliberately

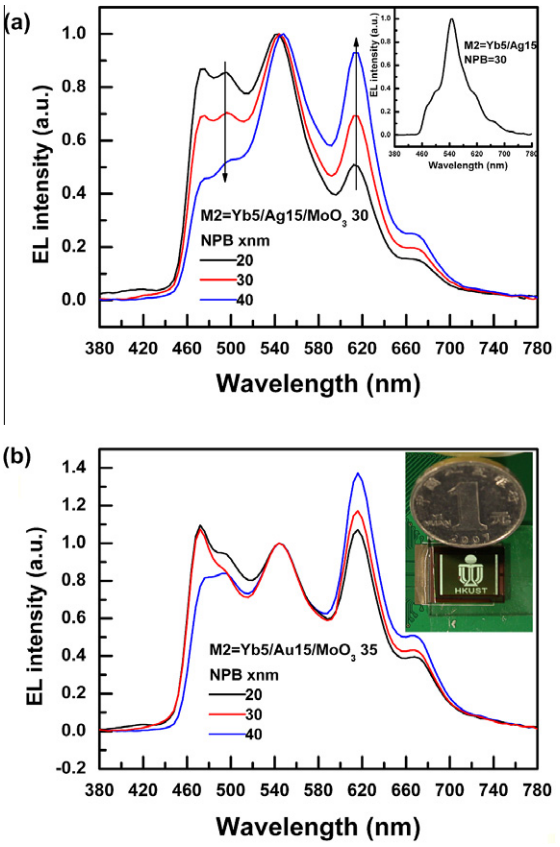

Fig. 4. (a) EL spectra of the devices with Ag based tri-cathode-layer. Inset shows the EL spectra of the devices with Yb (5 nm)/Ag (15 nm) top cathode. (b) EL spectra of the devices with Au based tri-cathode-layer. Inset shows a photo of the Si based SVGA+ microdispaly developed in this study. All devices were driven at 8 V for measuring the EL spectra.

by changing the thickness of NPB to further compare the interference effects of the cavity with different top cathodes. As shown in Fig. 4a, for devices with Ag based tri-cathode-layer, as NPB thickness increases, the blue emission decreases quickly while the red emission enhances rapidly, which may be attributable to the interference effects or shifting of the recombination zone. Also, the spectra exhibit slightly red-shift as the cavity length increases, a typical phenomenon in interference cavity. However, for the devices with Au based tri-cathode-layer, the white spectra only exhibit a slighted change as the increased of cavity length, which may be mainly caused by the shifting of the recombination zone. Noted that, both devices have the same emission and injection layers, thus the exciton recombination zone should also be identical. The severe change and red shifting white spectra as the increased of cavity length of the devices with Ag based tri-cathode layer are therefore most likely caused by interference effects; hence to obtain balanced white emission, one should carefully tune the thickness of the cavity length. While the relatively stable white spectra as the increased of cavity length of the devices with Au based tri-cathode-layer implies a much weakened interference effect; hence broadband white spectra with evenly separated R, G, B peaks and equal intensity are much easier to obtain, as shown in Fig. 4b. At NPB = 30 nm, the white spectra exhibit a CIE coordinate of (0.36, 0.42) and a high CRI of 85, rendering such top-emitting WOLEDs to be ideal candidate for display or lighting applications. We have successfully applied such top-emitting WOLEDs in the Si based microdisplay with SVGA+ resolution, as shown in Fig. 4b inset. It is noted that the emission color of the demonstrated top-emitting WOLEDs is not pure white and the CIE coordinate is far from (0.33, 0.33). To remedy this deficiency, deep fluorescent blue emitter like 4,4′-bis(9-ethyl-3-carbazovinylene)-1,1′-biphenyl (BcZVBi) may be employed to replace the sky blue emitter FIrPic [1].

The viewing characteristics of the white spectra are further examined. As shown in Fig. 5a, for the devices with Ag based tri-cathode-layer, the red emission decreases while the blue emission increases as the increased of viewing angle, mainly due to the reduction of cavity length viewed from an oblique angle. While the red emission remains unchanged regardless of the change of viewing angle for the devices with Au tri-cathode-layer as shown in Fig. 5b, again confirms a neglectable interference effect. However, the blue emission decreases as the increased of viewing angle, which is attributable to the strong absorption of the Au at the blue color region. At oblique angle, light see a thicker Au layer than that of their cousins at normal angle, thus leading to lower blue emission intensity at oblique angle. Fig. 5c and d show the EL spectra under different driving voltages. At high voltage, the exciton recombination zone shifts towards the green/red emission layer, thus one observes a decreasing blue emission and an increased red emission. The CIE coordinates changing from (0.34, 0.40) at 6 V to (0.36, 0.42) at 10 V for the devices with Au based tri-cathode layer.

Fig. 6 compares the key characteristics of the top-emitting WOLEDs with the Ag and the Au tri-cathode-layer. Both devices show similar current density–voltage–luminance and efficiency–luminance characteristics due to their identical structures; for example, both devices turn on at 3.8 V for 1 cd/m^2 and at ~7 V for 1000 cd/m^2, indicating that with the modification of Yb electron injection layer, Au works excellently as a cathode [17,23] despite its high work function. The devices with the Au based tri-cathode-layer exhibit a slightly higher efficiency than that of the devices with the Ag based tri-cathode-layer, which may be mainly due to the higher transmission of the Au based tri-cathode-layer than that of the Ag based tri-cathode layer [17]. For example, at a typical application luminance level of 1000 cd/m^2, the devices with the Au tri-cathode-layer demonstrate an efficiency of 23 cd/A and 10.5 lm/W, higher than 21 cd/A and 9.1 lm/W for the devices with the Ag based tri-cathode-layer. Further optimization, for example, electrical doping the charge transporting layer [24], employing new emitters/host with high carrier mobility and efficiency, applying out-coupling techniques [25,26], can be employed to boost the device performance.

4. Summary

In conclusion, the interference effects of the microcavity can be greatly alleviated by reducing the reflection of the

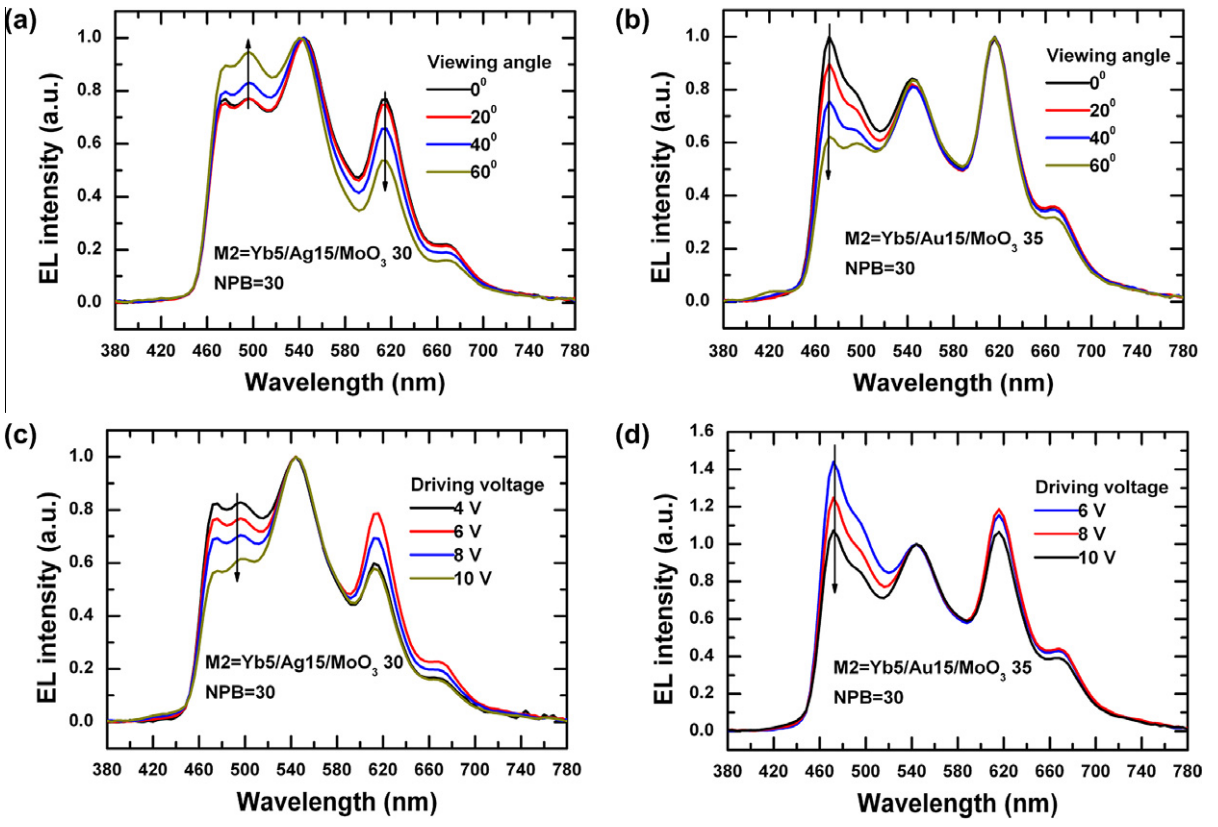

Fig. 5. (a) EL spectra of the devices with Ag based (a) and Au based (b) tri-cathode-layer at different viewing angle. EL spectra of the devices with Ag based (c) and Au based (d) tri-cathode-layer at different driving voltage.

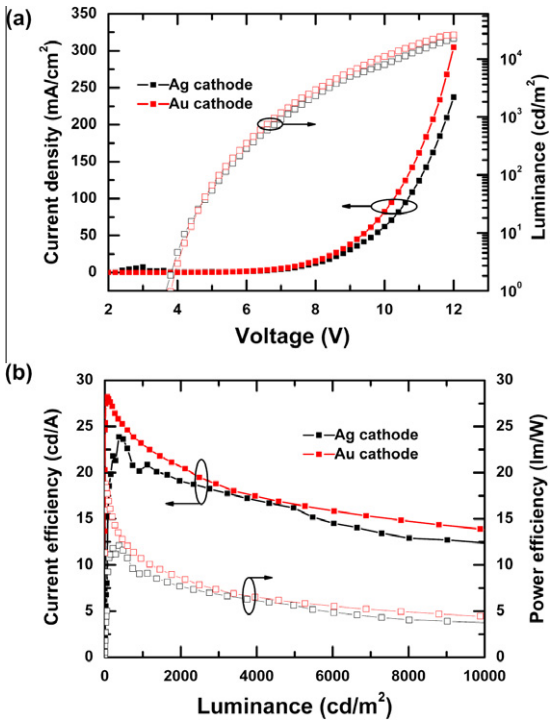

Fig. 6. Current density–voltage–luminance (a) and efficiency–luminance (b) characteristics of the devices with Ag and Au based tri-cathode-layer.

top cathode. Au, modified by a 5 nm Yb electron injection layer, can not only be an excellent cathode for injecting electrons, but also exhibits lower reflection and higher transmission than that of the mostly used Ag top cathode. By employing the low reflection Yb (5 nm)/Au (15 nm)/MoO_3 (35 nm) cathode, top-emitting WOLEDs with evenly separated R, G and B emission peaks have been demonstrated. At a luminance of 1000 cd/m^2, the top-emitting WOLEDs exhibit a CIE coordinate of (0.36, 0.42), a high CRI of 85 and an efficiency of 23 cd/A, 10.5 lm/W. As well, the spectra of the top-emitting WOLEDs demonstrate a very weak angle dependence due to the neglectable interference effects. The top-emitting WOLEDs demonstrated here, which have been successfully applied in the Si based microdisplay, would be an ideal candidate for high resolution active-matrix display or indoor lighting applications.

Acknowledgments

The authors thank Prof. Wai-Yeung Wong's group for providing the green-yellowish emitter **1**, and Mr. Pengfei Sun for driving the microdisplay panel. This work was supported by the Hong Kong Government Research Grants Council Grant Number 614410 and AOE/P0308PG2.

References

[1] S. Chen, G. Tan, W.-Y. Wong, H.-S. Kwok, White organic light-emitting diodes with evenly separated red, green and blue colors for

efficiency/color rendition trade-off optimization, Adv. Funct. Mater. doi:10.1002/adfm.201100895, 2011.
[2] S. Chen, H.-S. Kwok, Top-emitting white organic light-emitting diodes with a color conversion cap layer, Org. Electron. 12 (2011) 677–681.
[3] <http://www.emagin.com/oled-microdisplays/>.
[4] J.-J. Lih, C.-I. Chao, C.-C. Lee, Novel pixel design for high-resolution AMOLED displays with a shadow mask, J. Soc. Inf. Display 15 (2007) 3–7.
[5] C.-H. Chang, H.-C. Cheng, Y.-J. Lu, K.-C. Tien, H.-W. Lin, C.-L. Lin, C.-J. Yang, C.-C. Wu, Enhancing color gamut of white OLED displays by using microcavity green pixels, Org. Electron. 11 (2010) 247–254.
[6] T. Ishibashi, J. Yamada, T. Hirano, Y. Iwase, Y. Sato, R. Nakagawa, M. Sekiya, T. Sasaoka, T. Urabe, Active matrix organic light-emitting diode display based on "super top emission" technology, Jpn. J. Appl. Phys. 45 (2006) 4392–4395.
[7] S. Kim, S. Lee, M. Kim, J. Song, E. Hwang, S. Tamura, S. Kang, H. Kim, C. Kim, J. Lee, J. Kim, S. Cho, J. Cho, M.C. Suh, H. Kim, A 3.0-in. 308-ppi WVGA AMOLED with a top-emission white OLED and color filter, J. Soc. Inf. Display 17 (2009) 145–149.
[8] J. Cao, X. Liu, M.A. Khan, W. Zhu, X. Jiang, Z. Zhang, S. Xu, RGB tricolor produced by white-based top-emitting organic light-emitting diodes with microcavity structure, Curr. Appl. Phys. 7 (2007) 300–304.
[9] S.-F. Hsu, C.-C. Lee, S.-W. Hwang, C.-H. Chen, Highly efficient top-emitting white organic electroluminescent devices, Appl. Phys. Lett. 86 (2005) 253508.
[10] M. Mazzeo, F.D. Sala, F. Mariano, G. Melcarne, S. D'Agostino, Y. Duan, R. Cingolani, G. Gigli, Shapping white light through electroluminescent fully organic coupled microcavities, Adv. Mater. 22 (2010) 4696–4700.
[11] R.S. Cok, J.D. Shore, Microcavity white-emitting OLED devices, J. Soc. Inf. Display 17 (2009) 617–627.
[12] P. Freitag, S. Reineke, S. Olthof, M. Furno, B. Lüssem, K. Leo, White top-emitting organic light-emitting diodes with forward directed emission and high color quality, Org. Electron. 11 (2010) 1676–1682.
[13] M. Thomschke, R. Nitsche, M. Furno, K. Leo, Optimized efficiency and angular emission characteristics of white top-emitting organic electroluminescent diodes, Appl. Phys. Lett. 94 (2009) 083303.
[14] H. Kannp, Y. Sun, S.R. Forrest, High-efficiency top-emissive white-light-emitting organic electroluminescent devices, Appl. Phys. Lett. 86 (2005) 263502.
[15] M.-T. Lee, M.-R. Tseng, Efficient, long-life and lambertian source of top-emitting white OLEDs using low-reflectivity molybdenum anode and co-doping technology, Curr. Appl. Phys. 8 (2008) 616–619.
[16] G. Xie, Z. Zhang, Q. Xue, S. Zhang, L. Zhao, Y. Luo, P. Chen, B. Quan, Y. Zhao, S. Liu, Highly efficient top-emitting white organic light-emitting diodes with improved contrast and reduced angular dependence for active matrix displays, Org. Electron. 11 (2010) 2055–2059.
[17] G.Z. Ran, G.L. Ma, Y.H. Xu, L. Dai, G.G. Qin, Light extraction efficiency of a top-emission organic light-emitting diode with an Yb/Au double-layer cathode and an opaque Si anode, Appl. Optics 45 (2006) 5871–5876.
[18] X. Zhu, J. Sun, X. Yu, M. Wong, H.-S. Kwok, High-performance top-emitting white organic light-emitting devices, Jpn. J. Appl. Phys. 46 (2007) 4054–4058.
[19] T. Shiga, H. Fujikawa, Y. Taga, Design of multiwavelength resonant cavities for white organic light-emitting diodes, J. Appl. Phys. 93 (2003) 19–22.
[20] S. Han, C. Huang, Z.-H. Lu, Color tunable metal-cavity organic light-emitting diodes with fullerene layer, J. Appl. Phys. 97 (2005) 093102.
[21] C.-L. Lin, H.-W. Lin, C.-C. Wu, Examining microcavity organic light-emitting devices having two metal mirrors, Appl. Phys. Lett. 87 (2005) 021101.
[22] H. Benisty, H.D. Neve, C. Weisbuch, Impact of planar microcavity effects on light extraction – part I: basic concepts and analytical trends, IEEE J. Quantum Electron. 34 (1998) 1612–1631.
[23] S.L. Lai, M.Y. Chan, M.K. Fung, C.S. Lee, L.S. Hung, S.T. Lee, Applications of Ytterbium in organic light-emitting devices as high performance and transparent electrodes, Chem. Phys. Lett. 366 (2002) 128–133.
[24] K. Walzer, B. Maennig, M. Pfeiffer, K. Leo, Highly efficient organic devices based on electrically doped transport layers, Chem. Rev. 107 (2007) 1233–1271.
[25] C.-C. Liu, S.-H. Liu, K.-C. Tien, M.-H. Hsu, H.-W. Chang, C.-K. Chang, C.-J. Yang, C.-C. Wu, Microcavity top-emitting organic light-emitting devices integrated with diffuser for simultaneous enhancement of efficiencies and viewing characteristics, Appl. Phys. Lett. 94 (2009) 103302.
[26] Z. Wang, Z. Chen, L. Xiao, Q. Gong, Enhancement of top emission for organic light-emitting diode via scattering surface plasmons by nano-aggregated outcoupling layer, Org. Electron. 10 (2009) 341–345.